On the Five Submodels in Shock-Vortex Interaction

충격파-와동 간섭을 구성하는 다섯 가지 소모델에 대하여

Keun-Shik Chang[1], Se-Myong Chang[2]
장근식, 장세명

충격파-와동 간섭은 다양한 비선형 물리 현상을 포함한다. 그 중에서도, 충격파 분리와 충격파-충격파 간섭에 대해서는 잘 알려져 있는 반면, 미끄럼 층에서 반사되는 파동이나 관통 충격파 등에 대해서는 지금까지 적절한 연구가 이루어지지 못했다. 저자들은 복잡한 충격파-와동 간섭이 시간에 따라 몇 개의 국지적인 소모델 (submodels)로 귀착됨을 발견하였다. 이는 와동에 의한 충격파의 분리, 충격파-충격파 간섭, 충격파-미끄럼층 간섭, 와동 중심의 충격파 통과, 그리고 충격파-소와동 간섭이다. 이러한 5 개의 소모델은 탐구 범위 내에서 충격파-와동 간섭의 전체 구조를 구성한다.

1. Introduction

In the literature the shock-vortex interaction is regarded as a composite of two distant but complementary compressible flow elements, the nonlinear shock deformation (Chatterjee, 1999) and the far-field quadrupolar acoustic radiation (Weeks and Dosanjh, 1967): see Ellzey et al. (1995). The recent development of CFD (Computational Fluid Dynamics) has availed high-resolution schemes with their numerical results appearing as good as the experiment itself: for instance, compare Sivier et al. (1992) with Schardin (1957). However, the shock-vortex interaction phenomena, in general, are so complex that not all the picture elements in the experimental visualization or the irregular shapes in the numerical contour plots can be readily identified.

The objective of this paper is to categorize the shock-vortex interaction into five submodels, some of which have not much been reported in the literature. Although the weak waves are considered secondary physics, they are important since they can offer essential clues to some mysterious parts of the shock-vortex interaction. For example, the well-known quadrupole sound can be explained with weak waves such as reflected wave and transmitted shock.

2. Methods and Models

Double-exposure holographic interferometry and shadowgraphy are used for experimental visualization with a shock tube. Navier-Stokes equations are numerically solved at the same time for the same geometry, on the quadrilateral unstructured adaptive grid using a high-resolution upwind scheme. See Chang and Chang (2000) in detail on the experiment and the computation. The results of experiment and computation can be compared one by one at a given instant to assist comprehension.

In this paper, we solve two experimental problems and two conceptual problems:

---

1) 한국과학기술연구원
2) 서울대학교

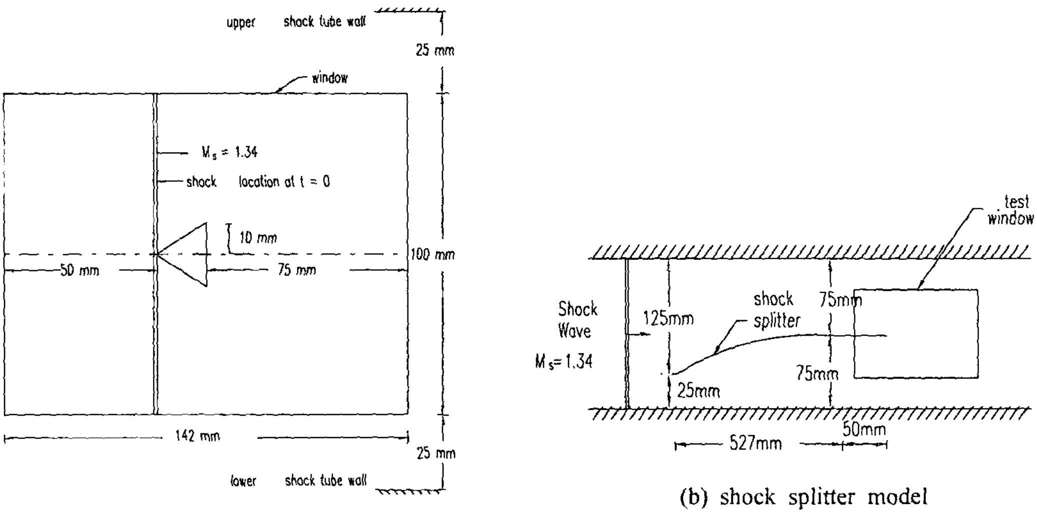

(a) Schardin's model

(b) shock splitter model

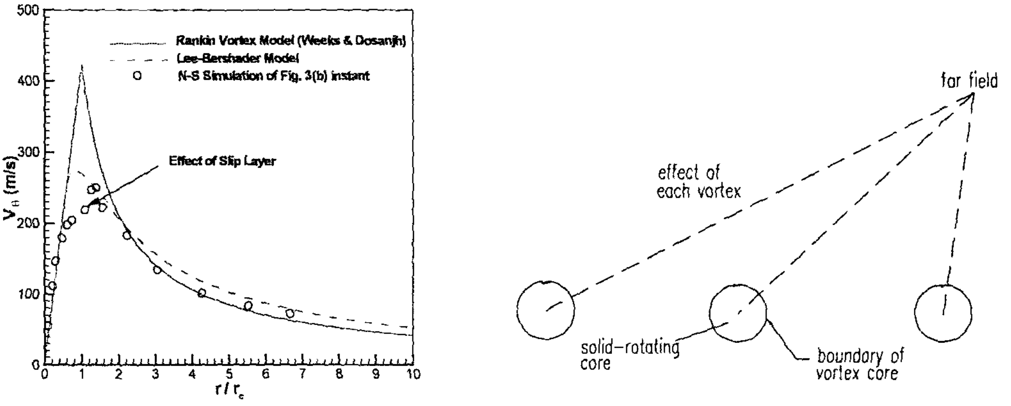

(c) single vortex model

(d) multiple vortex model

Fig. 1 Models in the present study.

2.1 Schardins Model

This problem is the modification of the Schardins experiment (1957). The planar shock of M_s=1.34 impinges to an equilateral triangular prism in Fig. 1(a). In the original experiment, the parasite waves reflected from the upper and lower wall polluted the test section, and therefore we used a smaller model. The side length is all 20 mm, and the prism or truncated wedge is fixed by the press of optical windows. The result of this experiment is counterchecked with Navier-Stokes simulation.

2.2 Shock Splitter Model

The shock splitter is a device to split a shock

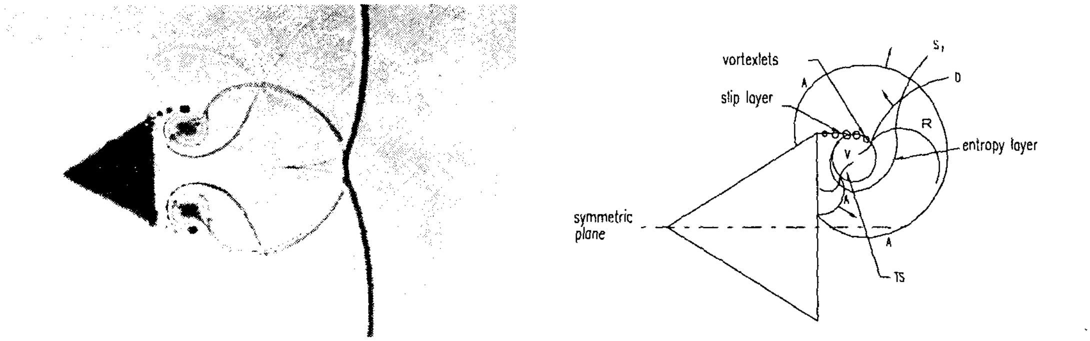

(a) Schardin's model: shadowgraph

(b) Schardin's model: sketch

Fig. 2 Submodel one: shock splitting.

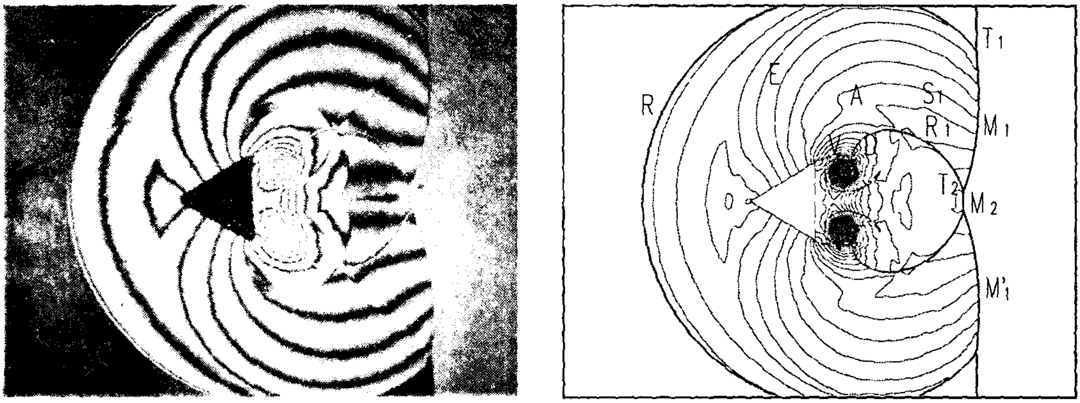

(a) Schardin's model: holographic interferogram.

(b) Euler simulation

Fig. 3 Submodel two: shock-shock interaction.

M_s=1.34 into two shocks, a faster (upper) shock M_s=1.41 and a slower (lower) shock M_s=1.22. The contour of this apparatus is designed with the method of characteristics induced by Whithams theory, and it is simply inserted in the shock tube: see Fig. 1(b). After the faster shock is diffracted at the sharp aft of the plat plate, the slower shock impinges to the vortex generated by the diffraction of faster shock.

2.3 Single Vortex Model

The vortex in the interaction is connected with a slip line in the experiment. Many conceptual vortex models include nonphysical terms to isolate the vortex. However, we used a primitive Rankin vortex model: see Fig. 1(c). The tangential velocity distribution is

$$V_\theta = \begin{cases} U_{\max}\dfrac{r}{r_c} & : 0 < r \le r_c \\ U_{\max}\dfrac{r_c}{r} & : r \ge r_c \end{cases} \qquad (1)$$

Other profiles such as pressure and density can be obtained from radial momentum conservation and adiabatic relation.

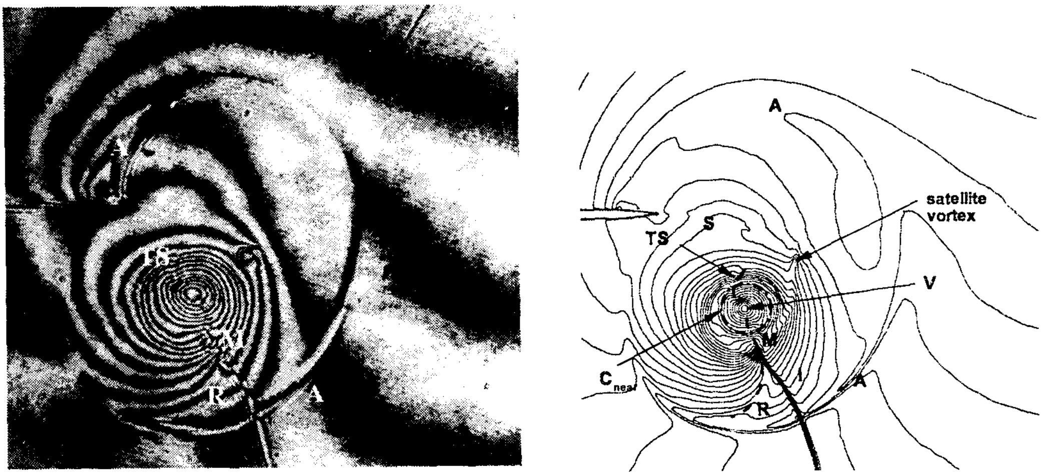

(a) shock splitter model: earlier stage (b) N-S simulation of (a)

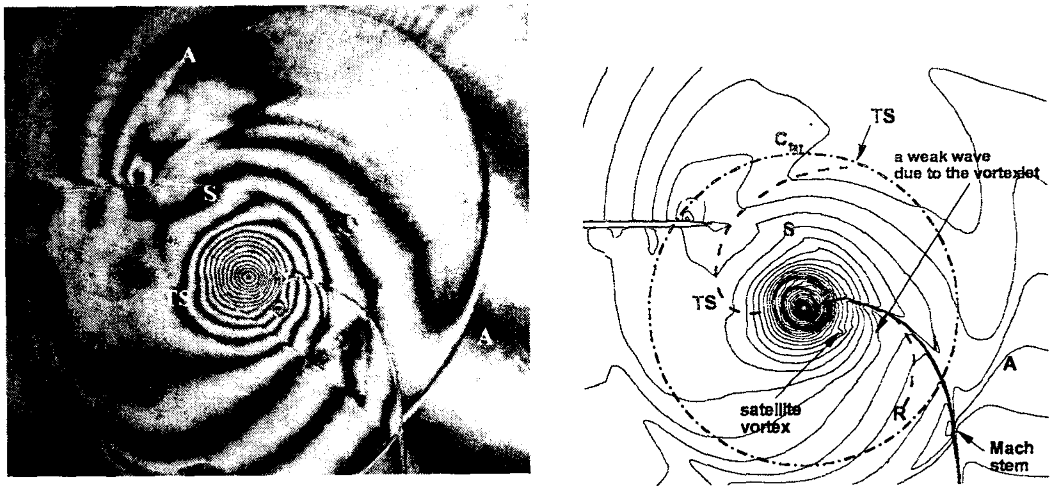

(c) shock splitter model: later stage (d) N-S simulation of (c)

Fig. 4 Submodel three and four.

2.4 Multiple Vortex Models

The single vortex model is extended using Foppls idea treating the vortex center as a singularity in Fig. 1(d). We assume a constant vorticity at each vortex core, and the core effect is superposed at far-field potential region. For n vortices located at $(x_{c,i}, y_{c,i})$ and core radius $r_{c,i}$,

$$V_\theta = \sum_{i=1}^{n} U_{\max}\frac{r_{c,i}}{r_i} \quad : r_i > r_{c,i} \qquad (2)$$

where

$$r_i = \sqrt{(x-x_{c,i})^2+(y-y_{c,i})^2}$$

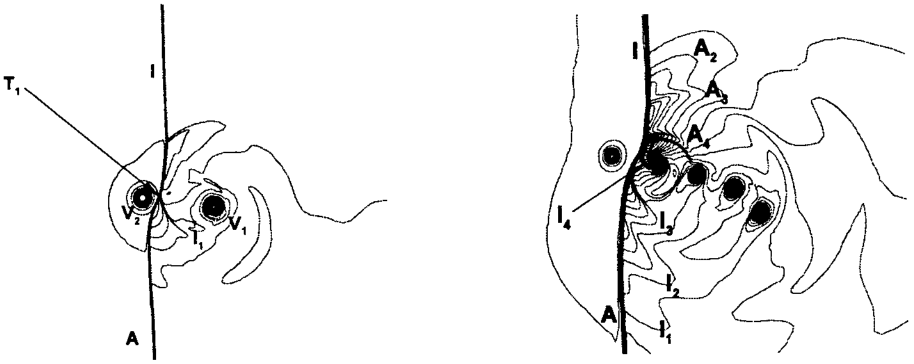

(a) two vortices model

(b) Five vortices model

Fig. 5 Submodel five: shock-vortexlet interactions

3. Five Submodels

3.1 Shock Splitting by the Vortex

As the impinging shock strikes the vortex, that segment of shock between the wall and the vortex center is rapidly deformed to a circular accelerated wave (A) in Fig. 2(a)-(b) due to the favorable vortex motion. The rest of the impinging shock held by the vortex center at one end is propagated slower due to the adverse vortex motion; thus the name 'decelerated shock (D)'. The acclerated wave (A) is not a pure shock wave but consists of two pairs of weak expansion and compression parts.

3.2 Shock-Shock Interaction

The decelerated shock (D) and the accelerated wave (A) can interact with each other as indicated in Fig. 3(a)-(b). The interaction is first regular but later changes to a Mach reflection (see M2 in Fig. 3(b)).

3.3 Shock-Slip Stream Interaction

The decelerated shock can interact with the slipstream itself on the outer edge of the vortex. In Fig. 4(a)-(d), a weak shock wave (R) is reflected while a Mach stem (M) is erected inside the vortex. Note the shock reflection can be either a compressive type (Fig. 4(a)-(b)) or an expansive type (Fig. 4(c)-(d)).

3.4 Shock Penetration through the Vortex Core

The Mach stem (M) does penetrate the vortex core to emerge as a new shock called the transmitted shock (TS) in Fig. 4(a)-(d). This pair of shock wave creates a quadrupolar pressure field in the vortex.

3.5 Shock-Vortexlet Interaction

The Navier-Stokes simulation has provided a very nice image of shock-multiple vortex interaction in Fig. 5(a)-(b). When the incident shock wave collides with the first vortex (*V1*), an accelerated wave (*A1*) is generated in Fig. 5(a) as also described in Fig. 2(b). The main shock wave (*I* and *A*) successively impinges into the adjacent vortex (*V2*). However, the structure is more complicated because the triple point (*T1*) opening two branches of shocks, A and A1, is now impinging into the vortex core. Therefore shock interaction with the second vortex and thereafter is necessarily associated with a double collision. The double structure of accelerated shock is henceforth resulted in the shock-multiple vortex interaction shown in Fig. 5(b).

4. Conclusion

We have found that the shock-vortex interaction is a complex phenomenon consisting of various asynchronous submodels. Five elementary interactions are identified in this paper among which the shock-slipstream interaction, the transmitted shock emerging from the vortex core, and the shock-vortexlet interaction are first indicated by the present authors. The penetrating and transmitted shocks through the vortex center are related with the quadrupolar acoustic radiation investigated by Weeks and Dosanjh (1967).

References

Chang SM, Chang KS (2000) On the Shock-vortex interaction in Schardins problem. Shock Waves, 10:333-343.

Chang SM, Chang KS (2000) Visualization of shock-vortex interaction radiating acoustic waves. Journal of Visualization, 3:221-228.

Chang SM, Lee S, Chang KS (2001) Reflection and penetration of a shock wave interacting with a starting vortex. AIAA Journal, *submitted.*

Chatterjee A (1999) Shock wave deformation in shock-vortex interaction. Shock Waves, 9:95-105.

Ellzey JL, Henneke MR, Picone JM, Oran ES (1995) The interaction of a shock with a vortex: shock distortion and the production of acoustic waves. Phys. Fluids, 7:172-184.

Hillier R (1991) Computation of shock wave diffraction at a ninety degree convex edge. Shock Waves, 1:135-144.

Schardin H (1957) High frequency cinematography in the shock tube. J. Photo Sci., 5:19-26.

Sivier S, Loth E, Baum J, Lohner R (1992) Vorticity produced by shock wave diffraction. Shock Waves, 2:31-41.

Weeks TM, Dosanjh DS (1967) Sound Generation by Shock-Vortex Interaction. AIAA J., 5:660-669.